Supporting Information

Void-rich layered $SiGe_x$ alloys via in situ molten salt electrochemistry for high-performance lithium-ion battery anodes

Xiaoyu Zhao[a], Ya Zheng[a], Wenhao Chen[a], Fei Zhou[a], Peng Huang[b], Tengyun Zuo[b], Qing Zhang[b*], Xi Liu[b], Juan Liu[c], Jian Liu[d], Jingwei Hu[a], Yongzhi Wang[a], Xiaocheng Li[a*]

[a]*Jiangxi Provincial Key Laboratory of Power Batteries & Energy Storage Materials, School of Materials Science and Engineering, Jiangxi University of Science and Technology, Ganzhou Jiangxi 341000, P.R. China*

[b]*Natural Resources Rights and Reserves Security Centre, Jiangxi Provincial Natural Resources Department, Nanchang, Jiangxi, 330025, P.R. China.*

[c]*Jiangxi Province Key Laboratory of Mining Engineering, School of Resources and environmental Engineering, Jiangxi University of Science and Technology, Ganzhou 341000, PR China*

[d]*Sunwoda Electronic-evb Co.,Ltd., Nanchang, Jiangxi 330044, P.R. China*

*Corresponding author: Xiaocheng Li (xiaocheng_li@jxust.edu.cn); Qing Zhang (29721960@qq.com)

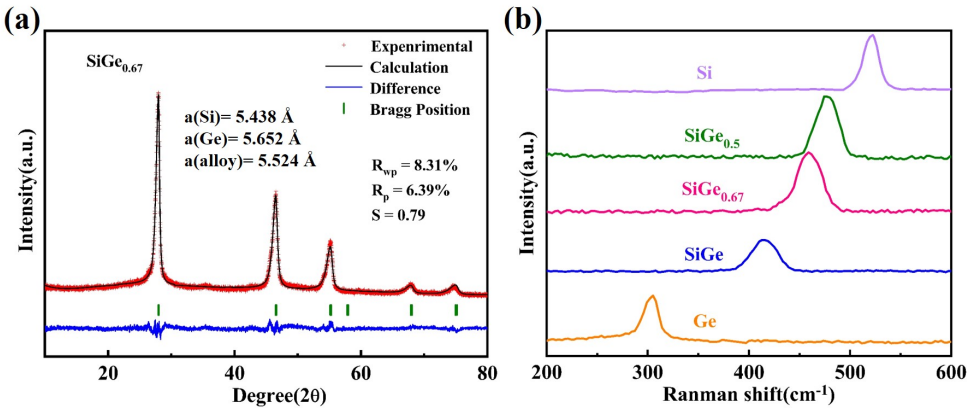

Fig. S1 (a) Rietveld refinement of XRD patterns for $SiGe_{0.67}$. (b) Raman results of Si, Ge and $SiGe_x$ alloys with various ratios.

Calculation of Ge Content from Refined Lattice Parameters Using Vegard's Law:

The refined lattice parameters are as follows: a(Si) = 5.438 Å, a(Ge) = 5.652 Å, and a(alloy) = 5.524 Å for the $SiGe_x$ sample. Applied the complete form of Vegard's law, which accounts for the total atomic fraction in the Si_1Ge_x system:

$$a(alloy) = \frac{1}{1+x} \times a(Si) + \frac{x}{1+x} \times a(Ge)$$

Solving this equation with the refined values yields a germanium content of x ≈ 0.67, corresponding to a composition of $SiGe_{0.67}$. This result, which provides a precise quantification of the Ge content.

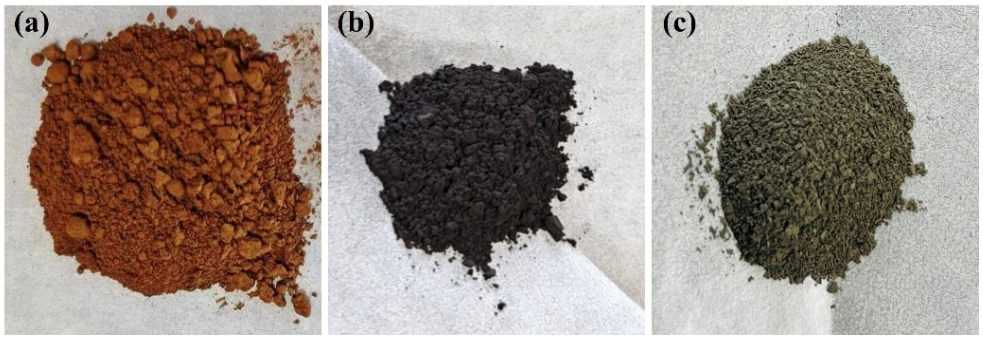

Fig. S2 Optical image of (a) Pristine SiO; (b) Ge powder; (c) Electrolysis product $SiGe_{0.67}$

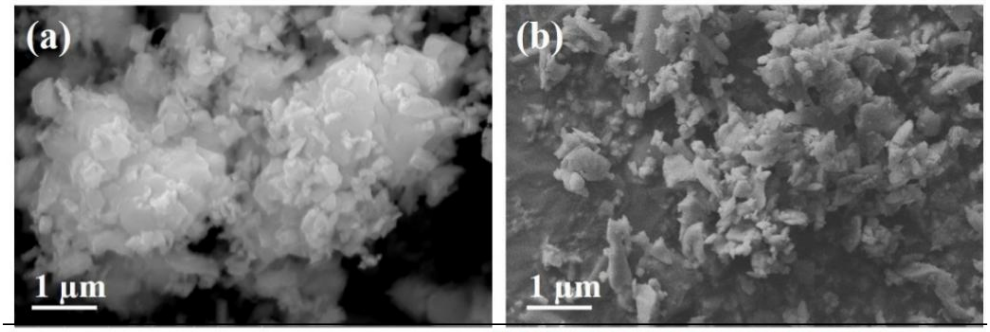

Fig. S3 SEM images of (a) Ge powder, (b) SiO particles.

Table S1 Atomic ratio of elements in $SiGe_{0.67}$

Element	Family	Atomic Fraction(%)	Atomic Error(%)	Mass Fraction(%)	Mass Error(%)	Fit error(%)
Si	K	59.41	7.76	37.01	3.08	0.33
Ge	K	40.59	7.29	62.99	9.78	0.14

Table S2 Comparison of the initial Coulombic efficiency and cycling stability of the $SiGe_{0.67}$ anode with other silicon-based composite materials.

Samples	**ICE(%)**	**Rate Performance (mAh g^{-1})**	**Cycling Stability (mAh g^{-1})**	**Ref.**
SiGe nanowire	86.8	625.5 @4 A g^{-1}	1500 after 270 cycles @1 A g^{-1}	S1
p-Si/CNT	52.8	532.4 @5 A g^{-1}	796 after 100 cycles @0.5 A g^{-1}	S2
Si@C@Si	52.8	1000 @1 A g^{-1}	904 after 100 cycles @0.5 A g^{-1}	S3
Si nanowire	76	521 @2 A g^{-1}	905 after 200 @1A g^{-1}	S4
porous Si@C	76.4	600 @4 A g^{-1}	630 after 100 cycles @0.84 A g^{-1}	S5
Si nanotube	76.4	1362 @5 A g^{-1}	950 after 200 @1 A g^{-1}	S6

$SiGe_{0.67}$	**82.6**	**610 @8 A g^{-1}**	**1190 after 200 cycles @1 A g^{-1}**	**this work**

DFT Calculation Methods:

We have employed the first-principles [7,8] to perform density functional theory (DFT) calculations within the generalized gradient approximation (GGA) using the Perdew-Burke-Ernzerhof (PBE) [9] formulation. We have chosen the projected augmented wave (PAW) potentials [10,11] to describe the ionic cores and take valence electrons into account using a plane wave basis set with a kinetic energy cutoff of 520 eV. Partial occupancies of the Kohn−Sham orbitals were allowed using the Gaussian smearing method with a width of 0.05 eV. The electronic energy was considered self-consistent when the energy change was smaller than 10^{-5} eV. A geometry optimization was considered convergent when the force change was smaller than 0.03 eV $Å^{-1}$. The Brillouin zone integration is performed using 3×1×1 Gamma centered grids k-point sampling for a structure.

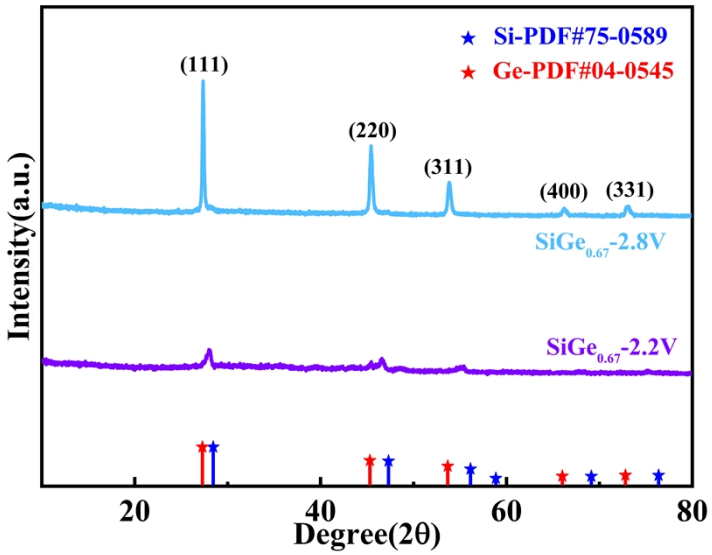

Fig. S4 XRD patterns of the electrochemical products obtained at different voltages.

The Li^+ diffusion coefficients D_{Li^+} calculation:

The Li^+ diffusion coefficients D_{Li^+} of the electrode is calculated based on eqns. (1) and eqns. (2):

$$D_{Li^+} = \frac{R^2T^2}{2A^2n^4F^4C^2\sigma^2} \quad (1)$$

$$Z' = R_0 + \sigma\omega^{-1/2} \quad (2)$$

where *R, T* and *F* stand for the gas constant, absolute temperature and Faraday constant, respectively. *A, n* and *C* signify the surface area of electrode, number of electrons per molecule during oxidation and concentration of lithium ions, respectively. The σ denotes the Warburg factor which can be fitted out based on linear curve of $\omega^{-1/2} \sim Z'$.

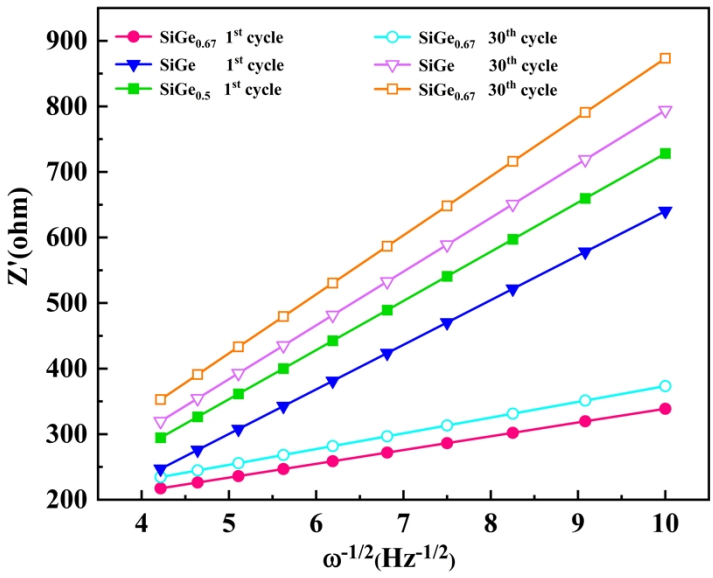

Fig. S5 The linear relationship of $\omega^{-1/2} \sim Z'$.

Table S3 Summary of the fitted value of EIS spectra

Sample	Cycles	R_{SEI} (ohm)	R_{ct}(ohm)	σ	$D_{Li}^{+}\times10^{-11}$ (cm^2 s^{-1})
SiGe	1st cycle	72.8	141.7	68	0.16
	30th cycle	110.2	170.3	82	0.11
$SiGe_{0.67}$	1st cycle	28.7	45.4	21	1.71
	30th cycle	47.1	56.8	24	1.31
$SiGe_{0.5}$	1st cycle	89.1	121.5	75	0.13
	30th cycle	142.4	180.6	90	0.09

References

[S1] X. Xu, X. Mu, T. Huang, A. Yu, Ge nanograin-enhanced Si/C composite anodes: anchored interfaces for rapid electron and ion conduction. J. Mater. Chem. A, (2025), Advance Article. DOI: 10.1039/D5TA05658F.

[S2] Q. Zhang, B. Xi, W. Chen, J. Feng, Y. Qian, S. Xiong, Synthesis of carbon nanotubes-supported porous silicon microparticles in low-temperature molten salt for high-performance Li-ion battery anodes, Nano Res. 15 (2022) 6184-6191

[S3] W. Weng, C. Zeng, W. Xiao, In Situ Pyrolysis Concerted Formation of Si/C Hybrids during Molten Salt Electrolysis of SiO2@ Polydopamine. ACS Appl. Mater. Interfaces, 11 (2019) 9156−9163.

[S4] Y. Dong, T. Slade, M. J. Stolt, L. Li, S. N. Girard, L. Mai, S. Jin, Low-Temperature Molten-Salt Production of Silicon Nanowires by the Electrochemical Reduction of CaSiO3. Angew. Chem., Int. Ed., 56 (2017) 14453−14457.

[S5] H. Dong, X. Fu, J. Wang, P. Wang, H. Ding, R. Song, S. Wang, R. Li, S. Li, In-situ construction of porous Si@ C composites with LiCl template to provide silicon anode expansion buffer, Carbon 173 (2021) 687-695.

[S6] F. Wang, Y. Ma, P. Li, C. Peng, H. Yin, W. Li, D. Wang, Electrochemical Conversion of Silica Nanoparticles to Silicon Nanotubes in Molten Salts: Implications for High-Performance Lithium-Ion Battery Anode. ACS Appl. Nano Mater. 4 (2021) 7028−7036.

[S7] G. Kresse, J. Furthmüller, Efficiency of Ab-Initio Total Energy Calculations for Metals and Semiconductors Using a Plane-Wave Basis Set. Comput. Mater. Sci., 6 (1996) 15−50.

[S8] G. Kresse, J. Furthmüller, Efficient Iterative Schemes for Ab Initio Total-Energy Calculations Using a Plane-Wave Basis Set. Phys. Rev. B, 54 (1996) 11169−11186.

[S9] J. P. Perdew, K. Burke, M. Ernzerhof, Generalized Gradient Approximation Made Simple. Phys. Rev. Lett., 77 (1996) 3865−3868.

[S10] G. Kresse, D. Joubert, From Ultrasoft Pseudopotentials to the Projector Augmented-Wave Method. Phys. Rev. B, 59 (1999) 1758-1775.

[S11] P. E. Blöchl, Projector Augmented-Wave Method. Phys. Rev. B, 50 (1994) 17953−17979.